Allysine modifications perturb tropoelastin structure and mobility on a local and global scale

Allysine modifications perturb tropoelastin structure and mobility on a local and global scale

Jazmin Ozsvar[a,b,c], **Anna Tarakanova**[d], **Richard Wang**[a,b], **Markus J. Buehler**[d] and **Anthony S. Weiss**[a,b,c,e,f]

***a* - Charles Perkins Centre,** *the University of Sydney, 2006 Sydney, NSW, Australia*
***b* - School of Life and Environmental Sciences,** *The University of Sydney, 2006 Sydney, NSW, Australia*
***c* - Cell Therapy Manufacturing Cooperative Research Centre,** *Adelaide, 5000, SA, Australia*
***d* - Laboratory for Atomistic and Molecular Mechanics (LAMM),** *Department of Civil and Environmental Engineering, Massachusetts Institute of Technology, Cambridge, MA 02139, USA*
***e* - Bosch Institute,** *The University of Sydney, 2006 Sydney, NSW, Australia*
***f* - Sydney Nano Institute,** *The University of Sydney, 2006 Sydney, NSW, Australia*

Correspondence to Anthony S. Weiss: *at: Bosch Institute, The University of Sydney, 2006 Sydney, NSW, Australia.*
tony.weiss@sydney.edu.au.
https://doi.org/10.1016/j.mbplus.2019.03.001

Abstract

Elastin provides elastic tissues with resilience through stretch and recoil cycles, and is primarily made of its extensively cross-linked monomer, tropoelastin. Here, we leverage the recently published full atomistic model of tropoelastin to assess how allysine modifications, which are essential to cross-linking, contribute to the dynamics and structural changes that occur in tropoelastin in the context of elastin assembly. We used replica exchange molecular dynamics to generate structural ensembles of allysine containing tropoelastin. We conducted principal component analysis on these ensembles and found that the molecule departs from the canonical structural ensemble. Furthermore, we showed that, while the canonical scissors-twist movement was retained, new movements emerged that deviated from those of the wild type protein, providing evidence for the involvement of a variety of molecular motions in elastin assembly. Additionally, we highlighted secondary structural changes and linked these perturbations to the longevity of specific salt bridges. We propose a model where allysines in tropoelastin contribute to hierarchical elastin assembly through global and local perturbations to molecular structure and dynamics.

Introduction

Elastin is the major elastic extracellular matrix (ECM) protein that is crucial for the mechanical resilience of elastic vertebrate tissues, including the skin, lungs and cardiovascular system [1,2]. The elastin polymer predominantly comprises its soluble subunit, tropoelastin [3], which is secreted by elastogenic cells and undergoes hierarchical self-assembly to form elastin fibers [4]. Assembly is initiated after secretion to the cell surface, where tropoelastin molecules rapidly form small spherules through a process termed coacervation [5,6]. These spherules are then deposited onto the microfibrillar scaffold within the ECM [7] where they assemble into robust, insoluble, and extensively cross-linked fibers [1].

The cross-linking of elastin is facilitated by one or more members of the family of lysyl oxidase (LOX) enzymes [8] and commences prior to deposition onto the microfibrillar scaffold [9,10]. As an amine oxidase, LOX modifies the ε-amino side chain of lysine to an α-aminoadipic δ-semialdehyde, resulting in an allysine residue [11,12]. Allysines are capable of undergoing spontaneous condensation with either the ε-amino groups of lysines or the semialdehydes

of other allysines, forming linear lysinonorleucine (LNL) or allysine-aldol (ALL) cross-links respectively [13]. LNL and ALL are able to condense further, forming larger, more complex cross-links such as desmosine or isodesmosine [14]. These four types of links are the most abundant cross-linked species within the mature elastin fiber [15,16].

The contribution of allysines to elastin assembly, other than purely their ability to form cross-links, is currently unknown. Elastin assembly is a finely tuned process relying on the intrinsic properties of tropoelastin, including the association of its hydrophobic domains and positioning of its cross-linking domains (Fig. 1), both of which are dependent on its molecular arrangement and flexibility [17–21]. The delicate balance between molecular arrangement and function can be perturbed by mutations that result in structural changes within both tropoelastin molecules and elastin fibers [1,17,20,21]. Thus, it is probable that the presence of allysines can also affect the conformation of tropoelastin, and in turn, influence coacervation and subsequent higher order assembly processes. To explore this, knowledge of allysine locations through cross-linking sites is needed to appreciate the spatial arrangement of molecules during coacervation and the overall steps by which elastin fibers are formed.

The precise cross-linking patterns within native elastin are only partially understood because the highly repetitive sequence of tropoelastin has hampered the mapping of specific cross-linking sites. More recently, utilization of enzymatic cleavage and mass spectrometry of native elastin has identified candidate regions involved in cross-linking [16,23,24]. Corroborating evidence for the involvement of these sites arises from further studies probing the *in vitro* cross-linking of synthetic recombinant human tropoelastin [25,26]. Despite advances in pinpointing cross-link locations, tropoelastin is a flexible molecule that retains its canonical shape [27], where this flexibility has rendered it difficult to accurately map these cross-linking sites to the tertiary structure of the molecule and impeded the use of traditional high resolution techniques to resolve its entire global structure [28]. As such, the only experimental shape data for tropoelastin are low resolution small angle x-ray scattering and small angle neutron scattering structures that comprise ensembles whose high resolution components were recently identified through molecular dynamics [20,21,29].

Recently, the full atomistic structure of tropoelastin was detailed as an ensemble using extensive replica exchange molecular dynamics (REMD) simulations [18]. The structure correlates remarkably well with the previous low-resolution structural data, and its secondary structural features are in accord with those indicated by circular dichroism and molecular mutation studies. These highlight the power of molecular dynamics (MD) in modeling flexible molecules. Examination of the molecule through normal mode analysis (NMA) also gave insight into the predominant global motions of tropoelastin that are likely to contribute to self-assembly [17,18], providing a molecular basis with which the effects of modifications within the scope of elastin assembly can be probed.

As the relatively flat energy landscape of flexible molecules, such as tropoelastin, allows them to transition between energy minima and take on a multitude of conformations, it is most appropriate to analyze flexible molecules as a structural ensemble. Principal component analysis (PCA) is being increasingly used to pinpoint and link structural variation to functionality within protein ensembles [30]. On this basis, PCA has been applied to wild type (WT) tropoelastin and has highlighted that despite its nature as a flexible molecule, its overall architecture fluctuates within a molecular ensemble that biased toward its canonical structure [27].

Here, we investigated whether allysine modifications are capable of altering the structure and

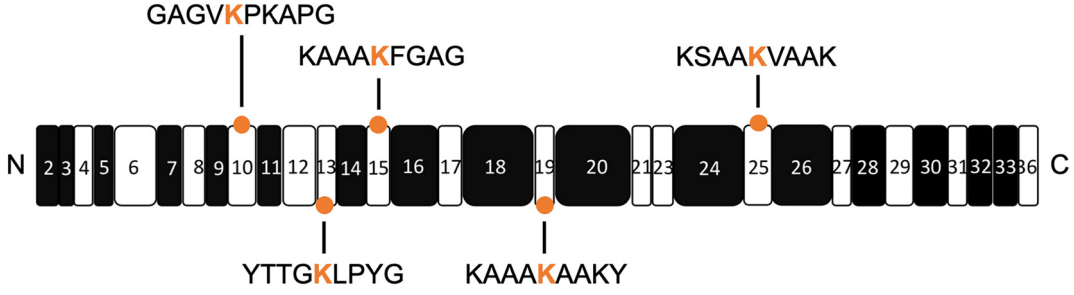

Fig. 1. Schematic representation of tropoelastin domains and allysines explored in this study. The hydrophobic and cross-linking domains are represented by the black and white boxes respectively. The N- and C-termini are denoted on either side of the schematic. The orange circles mark the domains containing allysine modifications in this study. The corresponding allysine (in orange) and their flanking amino acid sequences are depicted.
Adapted from [22].

dynamics of tropoelastin molecules. We conducted REMD to sample the conformational landscape of tropoelastin to understand the consequences of single and multiple allysine modifications. We focused on ensemble-based methods such as PCA to describe changes in overall structural variance and flexibility, local secondary structural changes and the mobility of specific residues. We also examined the intrinsically accessible molecular motions within the allysine containing molecules and investigate the contribution of salt bridges to the molecular changes. Our findings reveal that allysines do more than simply serve as static precursors to cross-links in elastin assembly, by contributing to changes in molecular structure and dynamics.

Methods

The methods for generating the WT model of tropoelastin have been previously described [18]. For single allysine modifications, residues 353 and 507 were selected for modification based on previous evidence for their involvement in and multiple references for cross-linking (Table 1). We used the modified molecules ALK353 and ALK507 to probe for changes tropoelastin may undergo subsequent to a single allysine modification. To understand the effect of multiple allysine modifications, we simultaneously modified residues from the aforementioned residues, as well as sites at 150, 199 and 239 in the protein, where these sites were based on prior characterization of native and synthetic elastin (Table 1) to give 5ALK. We restricted these changes to sites where multiple publications point to the sites of allysines. The rationale behind using 5ALK was that elastin is extensively cross-linked, and this allowed us to explore a representative construct where the majority of tropoelastin molecules contain more than one modification. The CHARMM22 force field [31] was selected due to its use in previous tropoelastin simulations [18]. Allysine was applied as a patch using parameters from the aldehyde functional groups of acetaldehyde and propionaldehyde from the CHARMM General Forcefield (CGenFF) [32] using Visual Molecular Dynamics (VMD) software [33].

Table 1. Summary of lysines residues converted to allysines in this study, their respective domains, and references to supporting studies.

Residue	Domain	References
150	10	[23,24]
199	13	[16,24–26]
239	15	[16,24]
353	19	[16,23–26]
507	25	[16,23–26]

The modified molecules were first simulated with NAMD [34] using implicit solvent replica exchange molecular dynamics (REMD). The implicit solvent step was intended to accelerate sampling time, as the water molecules of explicit solvent are a major limitation in REMD. Each molecule had a total of 48 replicas distributed exponentially over a temperature range of 280–480 K, giving an exchange acceptance frequency between 0.2 and 0.3. Exchanges were attempted every 1 ps and were accepted based on the Metropolis criterion described in previous REMD studies [18]. Non-bonded forces were applied with cut-off of 16 Å, a switch distance of 14 Å and a pair distance list of 18 Å. Implicit solvent was simulated using a dielectric constant of 80, ion concentration of 0.15 M, and an alpha cut off of 15. A total of 5.2 ns was simulated per tropoelastin molecule, with ~ 240 ns total simulation time for the entire ensemble across all temperatures of each molecule.

The root mean square deviation (RMSD) of atomic fluctuation was used as an indicator of structural convergence. Upon reaching convergence, 1000 structures were extracted from the last 2 ns of the 310 K replica and clustered by k-means analysis with the MMTSB toolkit [35] using a RMSD of 5 Å. MMTSB was used to determine the distribution of clusters generated by k-means analysis and the most representative structures of the most populated clusters. The ProDy package [30] was utilized to construct anisotropic network models (ANM) and principal component analysis (PCA) on the ensemble of each molecule. In-house Tcl/Tk, R and Matlab scripts were used for all other analyses.

The average structure of the most populated cluster for each molecule was further equilibrated in explicit aqueous solvent. A cubic box containing ~100,000 water molecules was used to solvate tropoelastin, while a padding distance of 20 Å from the molecule's edges was used to ensure the protein would not contact itself through the periodic boundaries of the water box. The box was neutralized with sodium and chloride ions at the physiological concentration of 0.15 M. After a brief minimization of the structure with the conjugate gradient method and equilibration in a constant volume system, the molecules were simulated with classical molecular dynamics in constant pressure systems using a time step of 2 fs. Equilibration was assessed using the RMSD of each structure, resulting in equilibration times of 100 ns, 130 ns and 230 ns for ALK507, ALK353 and 5ALK respectively. A temperature of 310 K was maintained by Langevin dynamics, with a damping coefficient of 1/ps. A constant pressure of 1 atm was applied using the Nosé-Hoover Langevin barostat with a period of 200 fs and a decay of 100 fs. For simulating non-bonded parameters, a cutoff of 12 Å was used, with a switch distance of 10 Å and a pair distance list of 13.5 Å. Electrostatics

were regulated by a Particle Mesh Ewald summation with a grid spacing of 1 Å. The resultant structures were used to conduct NMA using elastic network models with ProDy [30] and VMD [33] using the NMWiz plugin.

Results

Allysine modified tropoelastin displays heightened structural variability over WT

We conducted ensemble analysis on 1000 structures that were derived from the last 2 ns of REMD simulation per molecule. We examined the structural variance within the ensembles through the contribution of the top 20 principal components (Fig. 2, **a-c**). It had been previously noted that 42% of the variance in WT is captured by the top principal components [27], and here, the two principal components accounted for 31–41% of the structural variance of the modified molecules. The sum of the variance of the top three principal components of these molecules ranged between 40 and 52% in comparison to 53% of the top three principal components of the WT. Additional principal components would be required for equating structural variance between allysine modified molecules compared to WT, so this indicated that the allysine containing molecules exhibited a higher degree of structural variability relative to WT when examined through these top principal components.

In addition to PCA, we conducted k-means clustering of proteins based on similarity of the root mean square deviation (RMSD) of atomic coordinates in Cartesian space. This type of clustering has previously demonstrated that WT favored a specific configuration over other structures within its ensemble [27]. There was a similar tendency with ALK353 and ALK507, where this trend changed with multiple allysine modifications (Fig. 2, **d-e**). On this basis, 5ALK displayed a relatively even distribution of structures throughout its top nine clusters, and was most evident through clusters 3 to 9, which each comprised between 68 and 81 structures (Fig. 2, **f**) and was consistent with a model where these structural clusters contributed to a comparable extent in 5ALK.

The relevance of the representative structures from the k-clusters was assessed by overlaying onto 3D PCA plots that describe PC1-PC2-PC3 space (Fig. 2, **g-i**). The most representative structure from the top 4 most populated k-clusters (depicted in red) within each ensemble were located within dense clusters on the PCA plots. This was also observed

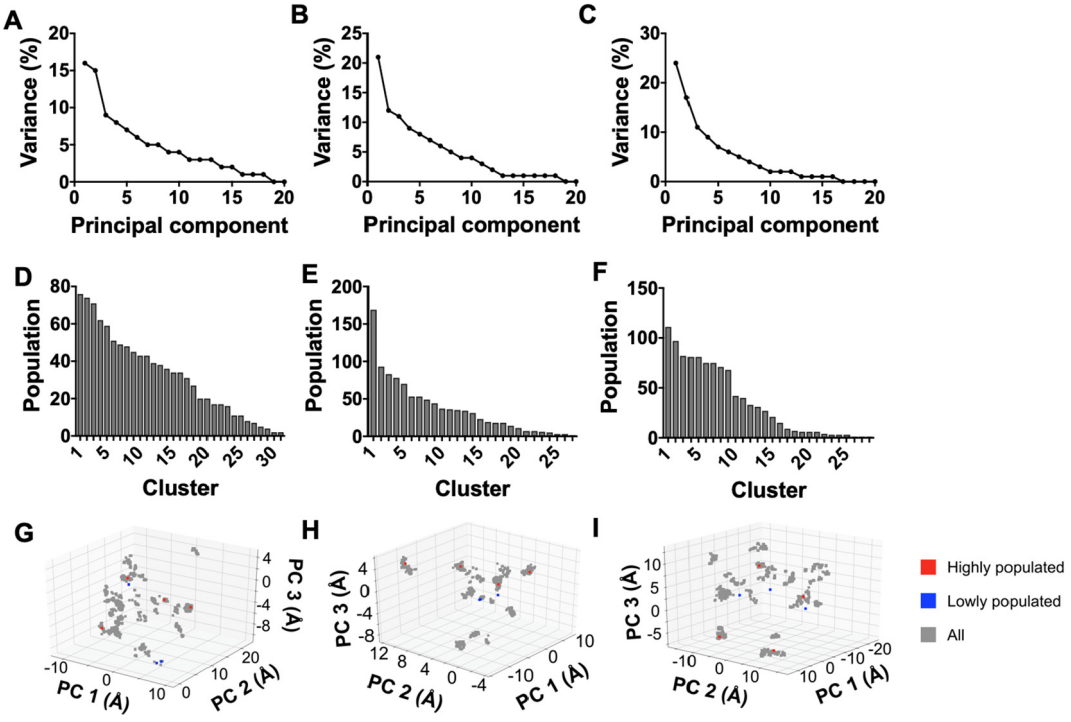

Fig. 2. Variance of the top 20 modes of principal component analysis of the structural ensembles for: A) ALK353, B) ALK507, and C) 5ALK. Distribution of structures arranged from most to least populated k-clusters using RMSD for: D) ALK353, E) ALK507, and F) 5ALK. The most representative structures from the k-clusters are overlaid onto PC1-PC2-PC3 space for G) ALK353, H) ALK507 and I) 5ALK. Representative structures are classed as either from most populated k-clusters (red squares) or least populated k-clusters (blue squares).

with WT [27]. Representative structures from the three least sampled ensembles were also overlaid onto the PCA plot, where they were found to reside in less populated areas. Most of these clusters were distinct, confirming that the 3 principal components neatly discretized structural differences between molecular k-clusters.

The 2D PCA plots showed less clustering resolution as evidenced by candidate structures from the least sampled conformations that resided in areas similar to the most accessible structures within PC1-PC2 space (data not shown). This was expected because the amount of structural variance of the allysine containing molecules accounted for by PC1-PC2 differed when compared to WT, as discussed above. This pointed to the need to proceed with at least the 3 top PCA components.

Converting lysine to allysine perturbs the global structure and intrinsic dynamics of tropoelastin

We used the sum of principal component modes to assess the mobility of allysine-modified tropoelastin ensembles by calculating the square displacement in Cartesian space of all alpha carbons in the protein backbone (**Supplementary 1, a-c)**. As only the top six principal component modes dominated the structure [27], we compared the sums of the top 2, 3, 6 or 20 principal component modes. We then identified that a minimum of three PCA modes describes the allysine containing ensembles. We found that although the combination of the top 2 and 3 modes substantially overlapped, the top 2 modes differed from the overall trend in combinations of higher modes in some domains (**Supplementary 1, a-c**). This feature differed from the WT ensemble, where there is good overlap of the top 2 and 3 modes [27].

Based on this, we examined structural similarities between WT and allysine modified tropoelastin by considering the overlap of the top 6 PCA modes between the different ensembles. We found only a mild correlation between WT and singly-modified tropoelastin (Fig. 3**, a-c**). Principal components 1, 3 and 5 of WT respectively correlated with the principal components 1, 3 and 1 of ALK353 (34–45%) (Fig. 3**, a**), whereas principal components 1 and 2 of ALK507 correlated with principal components 2 and 3 of WT (29–40%) respectively (Fig. 3**, b**). In contrast, principal components 3 and 5 from 5ALK

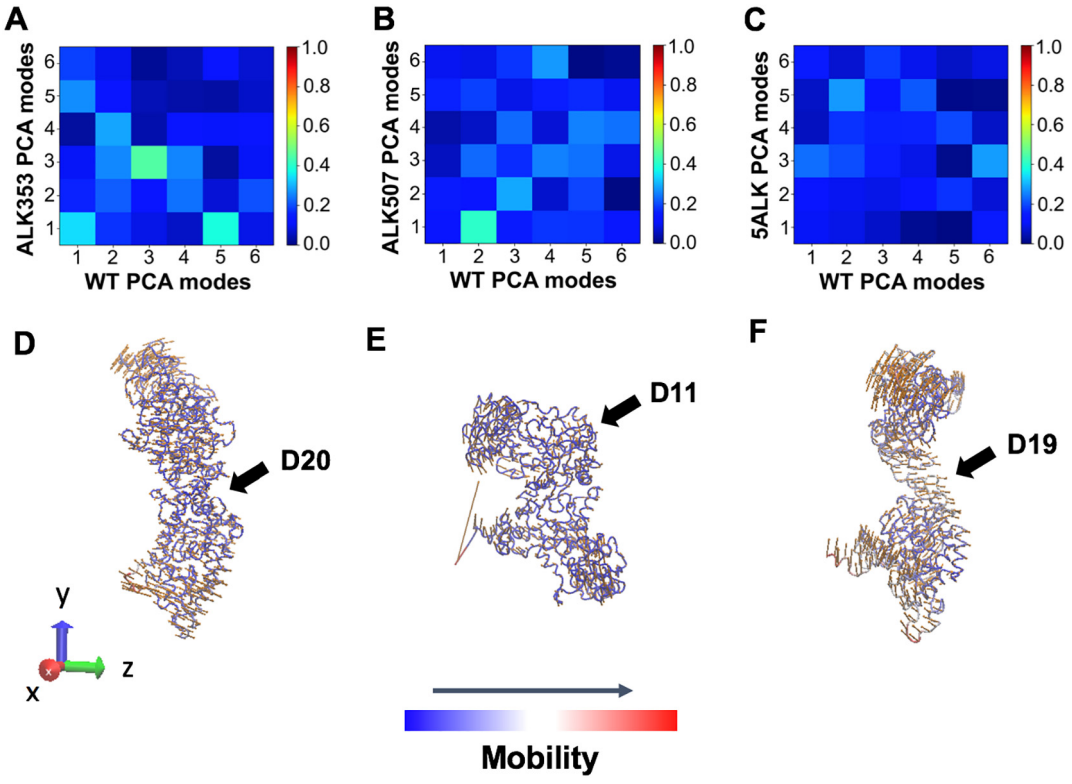

Fig. 3. Heatmap comparisons of the top 6 principal component modes for WT with A) ALK353, B) ALK507, and C) 5ALK. Normal mode analysis images that combine the 6 most accessible modes of the most representative structures for: D) ALK353, E) ALK507, and F) 5ALK. Directionality and magnitude of the modes are depicted in orange. The gradient bar depicts mobility, where red corresponds to the most mobile regions. Black arrows indicate domains that act as hinges.

weakly (< 22%) correlated with 2 and 6 from WT (Fig. 3, **c**). As the PCA modes relate to the overall architecture of a molecule, this indicated a potential shift away from the canonical structure. Comparisons between the allysine-modified molecules also revealed low similarities (< 45%) between principal components of the ensembles, indicating that the locations of the allysine modifications led to different structural consequences (**Supplementary 1, d-f**). This model was supported by the addition of allysines which shifted the structural ensemble from the WT structure (**Supplementary 2, a-c**). We found that the extent to which average structures departed from WT depended on the location and extent of these modifications. For example, ALK353 was globular and displayed a C-terminal foot region that pointed down from the protein's center (**Supplementary 2, a**), whereas ALK507 was slightly more compact along its vertical axis and displayed a preference for a C-terminus that was raised toward the center of the protein (**Supplementary 2, b**). Relative to WT, 5ALK revealed a compacted C-terminus and an extended molecular body (**Supplementary 2, c**).

To explore how these changes in global molecular shape affected the motions intrinsically accessible to the molecule, we employed NMA using anisotropic network models (ANMs). ANMs are useful in explaining global molecular motion as they are reliant solely on the architecture of the molecule, rather than localized secondary structures, and encompass those motions most accessible to WT including a twist in the N-terminus with a scissors motion in the C-terminus [18,27]. NMA was used to describe representative solution structures from the most populated k-cluster of each ensemble. On combining the lowest 6 normal modes of movement, the scissors-twist motion was observed in ALK507 but not in ALK353 or 5ALK (Fig. 3, **d - f**). We propose that the scissors-twist motion relies on the C-terminus adopting a configuration with two protruding feet as seen in WT and ALK507.

ALK353 displayed N- and C-terminal flexibility about domain 20, which acted as a hinge, with additional C-terminal pivot on the plane orthogonal to domain 20 (Fig. 3, **d**). The N-terminus ALK507 demonstrated flexibility about a hinge formed by domain 11 and was the only modified molecule that presented a scissors twist in its foot region (Fig. 3, **e**). The N- and C-termini of 5ALK moved about domain 19, which acted as a hinge in this molecule (Fig. 3, **f**). Taking into account that allysine-containing structures exist soon after LOX modification, this suggests a combination of these movements contributes to assembly.

Allysines alter the conformational sampling of domains

We compared fluctuations of the protein backbone in WT and allysine modified tropoelastin for the 6 top principal component modes. ALK353 and ALK507 departed from WT with markedly differing regions of high and low mobility (Fig. 4, **a-b**) [27] with decreases in the overall magnitude of fluctuation throughout, accompanied by dampened mobility in domains 19 and 25 which comprised the allysine modifications in ALK353 and ALK507 respectively.

In contrast, the magnitude of fluctuations in the 5ALK backbone had increased over WT, meaning that the molecule was more flexible (Fig. 4, **c**). We noted that the mobility pattern within 5ALK was closer to that seen for WT than to either ALK353 or ALK507, where high mobility domains within WT were also mobile in 5ALK, specifically domains 2–5 (residues 1–51), domains 10–19 (residues 133–357) and domains 21–23 (residues 413–445) (Fig. 4, **c**). As tropoelastin requires multiple allysines prior to forming elastin, 5ALK serves as a model of functionally significant oxidized tropoelastin in elastogenesis, so its similarities in mobility to WT were considered salient and are sequentially considered here.

Domains 2–5 are located at the head of both WT and 5ALK through domain 6 where they are accompanied by salt bridges [18,20]. The importance of domain 6 in elastogenesis is demonstrated by the formation of markedly altered fiber morphology when tropoelastin's sole aspartate is mutated to alanine [20]. This suggests that the role of domain 6 in elastin maturation is to hold domains 2–5 in place, potentially for head-to-tail assembly as previously proposed [29]. Our data are consistent with these findings because domain 6 remained stable relative to its flanking domains (Fig. 4, **c**).

We note that domains 10–19 undergo high conformational sampling in both WT and 5ALK, which is credited to contributions to entropy-based extensibility by this part of the molecule [36]. In 5ALK these regions are mobile relative to the N-terminal half of the molecule.

Domains 21–23 display high fluctuations within WT and 5ALK (Fig. 4, **c**). Their flexibility as seen in previous molecular dynamics studies is proposed to facilitate cross-linking [24]. Experimentally these same domains were identified as cross-linking hot spots *in vitro* [25,26] and found as cross-links in native elastin [16,24]. Our data help to explain these findings, by identifying that the mobility of domains 21–23 enhances LOX-mediated modification and subsequent cross-linking.

Also relevant is that domain 36 in 5ALK (Fig. 4, **c**) undergoes high conformational sampling similarly to WT [18,27]. Consistent with observations here, this domain contains a cell-interactive region [37,38] and has been established as particularly flexible in previous elastic network models and by NMA [17,39]. It has been proposed that the C-terminus plays a role in positioning the molecule during aggregation and eventually cross-linking [40], features which are in accord with higher regional mobility as seen here.

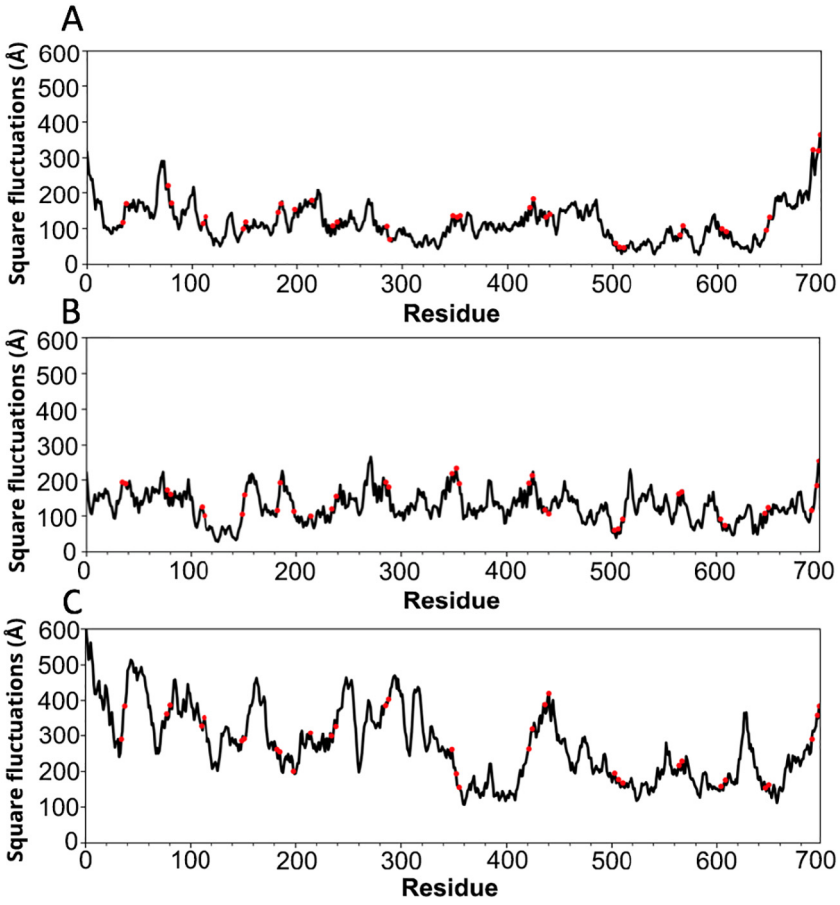

Fig. 4. Protein backbone square fluctuations as a combination of the top 6 principal component modes for: A) ALK353, B) ALK507, and C) 5ALK. Lysines and allysines are depicted as red dots.

We also note (Fig. 4**, a-c**) that the number of lysines and allysines located in regions of high displacement (80–85%) is similar to that reported for WT (83%), as expected for a model where these residues continue to sample the conformational landscape in order to facilitate further modifications and ensuing cross-links.

Allysines facilitate changes in salt bridges that contribute to structural variance and lead to local secondary structural changes

To explore mechanisms behind the heightened flexibility and conformational changes caused by allysine modification, we examined the presence of salt bridges. It is well accepted that tropoelastin's three negatively charged residues (D72, E345 and E414) are involved in maintaining its overall structure [18,20,21]. By converting lysine to allysine, the positive charge is lost, rendering them incapable of forming salt bridges. On this basis, we noted changes in salt bridge binding that impacted upon the structural modifications, through PCA and displayed altered conformational sampling. WT was capable of forming multiple salt bridges through all three negatively charged residues for a substantial proportion of the time sampled (Fig. 5**, a**). In contrast in 5ALK, not only did the salt bridge patterns change, but salt bridge longevity decreased (Fig. 5**, b**). Considering the higher magnitude of protein backbone fluctuation displayed by 5ALK (Fig. 4**, c**), it is likely that these conversions from lysines to allysines released tropoelastin from a more stable configuration and accordingly conferred increased mobility. This model is consistent with our previous observation that there was less overall dominance of a single cluster in the entire structural ensemble (Fig. 2**, f**), because less salt bridges would lead to a regional freeing of the molecule and increase its ability to locally sample other states.

We examined the local secondary structural effects of allysines within their respective domains. It has been previously noted that changes in α-helicity within domains have a tendency to predispose them to stiffness and alter the collective motions of the molecule [18]. The α-helical content

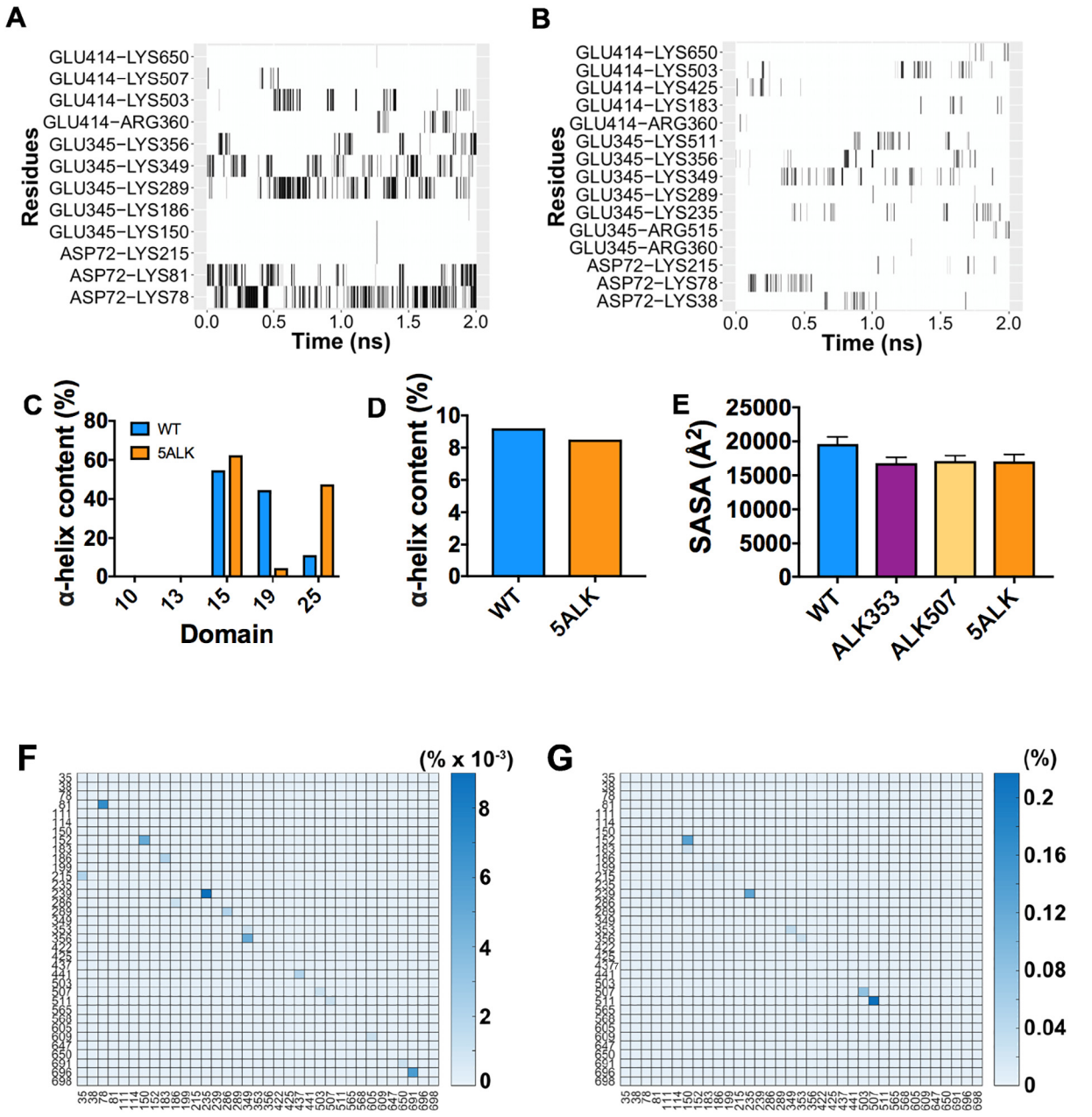

Fig. 5. Salt bridge contact maps for: A) WT and B) 5ALK, where salt bridge presence and longevity are indicated by black bars. The percent transient α-helical content of WT and 5ALK is shown in C) specific domains and D) the entire molecules. E) Displays the solvent accessible surface areas of hydrophobic domains globally. Distance maps are shown for lysines and/or allysines in: F) WT and G) 5ALK, where the gradient depicts increasing time spent in close proximity (4.7 Å) to nearby lysines and/or allysines.

of domains 19 and 25 exhibited substantial changes (Fig. 5**, c**), yet the overall α-helicity of the molecules did not significantly differ (Fig. 5**, d**). The lack of change at a global secondary structural level was consistent with a requirement for flexibility in self-assembly [19,41]. Additionally, when considering the previously discussed differences in overall tropoelastin mobility, the maintenance of global structure highlighted potential differences between disease-associated mutations [18,20,21] and natural functional modifications.

Hydrophobic solvent accessible surface area decreases in the presence of allysines

The total solvent accessible surface area (SASA) of the hydrophobic domains was calculated for all molecules. A decrease from the previously

published SASA of 196.24 nm^2 for WT [18] to 168.02–171.20 nm^2 for the modified molecules was observed (Fig. 5, **e**). This compared with changes in the accessibility of hydrophobic regions at the same scale of those observed for two previously modeled tropoelastin mutations, D72A and G685D [18]. As the exposure of hydrophobic regions is known to drive coacervation, this would be explained by decreased salt bridges and increased mobility of the molecule, which allows hydrophobic regions to bury further inside the modified molecules than seen in WT.

Distances between residues decrease upon allysine modification

In addition to forming intermolecular cross-links, tropoelastin is also known to form multiple intramolecular cross-links [16,24]. Approaching positive charges on juxtaposed lysines tend to repel, so it is logical that conversion to the neutral allysine reduces the distance between C_ε and C_δ groups of these residues [24]. Our study is consistent with these findings, as we established that the presence of allysine facilitates an increase in the proportion of time spent in proximity (4.7 Å) to its neighboring lysines when WT and 5ALK are compared (Fig. 5, **g-f**).

Discussion

Allysine formation is an essential step in making elastin from tropoelastin, yet its molecular effects have not previously been considered. This study is the first to demonstrate that structural changes arise from allysine modifications. Converting lysine to allysine alters structural ensembles, changes the mobility and accessibility of domains, and varies accessible molecular motions of tropoelastin.

It is well accepted that the structure and functionality of tropoelastin are substantially affected by single point mutations [18,20,21]. Although deviations from WT structure are generally linked to disease states [40], here, we demonstrate that naturally occurring modifications are also capable of altering WT structure. We established that structures within the ensemble depart from the canonical WT shape with progressing modifications. This departure is of biological relevance, as the structural consequences of allysines had not been fully explored within the context of elastogenesis. Furthermore, we highlighted the decrease in dominance of a single set of structures with progressing allysine modifications. These findings are in accord with recent mass spectrometry data and help to explain the heterogeneity of elastin cross-linking [16]; we posit that decreased structural dominance contributes to this heterogeneous cross-linking because 5ALK more evenly samples a range of structures.

Tropoelastin's mobility is crucial to its functionality and also plays a significant role in self-association [19,41]. Here, it was demonstrated that allysine-modified tropoelastin displayed altered mobility relative to WT in key domains. This effect was assisted by sparse, short-lived salt bridges that resulted in local and global secondary structural changes. The high conformational sampling of WT most likely facilitates rapid aggregation and LOX mediated modification [27] however, we propose that the altered mobility patterns within ALK353 and ALK507 could serve as a checkpoint required prior to further assembly. Considering elastin's known extensive cross-links and functionality, this checkpoint limits participation by molecules lacking sufficient allysines and reduces the probability of their incorporation into the growing elastin chain where they would form a weakly cross-linked fiber. This checkpoint model is supported by the known presence of lysines in relatively mobile regions of tropoelastin that are recognized as important in cross-linking [16,23,24,42]. Further support for the checkpoint model arises when considering the time frame of elastin assembly. Tropoelastin molecules cross-link subsequent to aggregation, which occurs after LOX has completed modification and dissociated from tropoelastin. This study benefits from the fact that tropoelastin structures organize on the order of nanoseconds, whereas coacervation occurs on the order of seconds [43], which means that assembly into elastin is at least several orders of magnitude slower than the time scales examined here. This indicates that allysine containing tropoelastin transitions away from the canonical tropoelastin shape prior to aggregation and cross-linking. However, the contribution of allysines to mobility is likely to change once tropoelastin is cross-linked due to restrictions imposed by the resultant bond. Further molecular dynamics studies could be undertaken to explore the effect of cross-linking on the mobility of allysine containing tropoelastin.

The current head-to-tail model of elastin assembly is based on the mapping of a handful of cross-links [23] onto the low resolution structure of WT [29]. ANMs based on the global architecture of WT have implicated the C-terminal scissors twist motion as being crucial to head-to-tail assembly [18]. The presence of the scissors twist in ALK507 further verified its importance in self-association steps. However, our ANMs of ALK353 and 5ALK displayed a loss of the C-terminal twist, unexpectedly indicating that these previously unexplored motions are also likely to contribute to higher order assembly.

The hydrophobic domains of tropoelastin dominate and drive tropoelastin association [1] and a decrease in SASA is associated with altered coacervation [18]. We propose that the lowered

SASA of allysine-containing tropoelastin contributes to the formation of aggregates that LOX can penetrate and further modify. This type of aggregate would therefore be an experimentally unexplored component in higher order elastin assembly that is testable *in vivo*.

A limitation of the current study is that only one allysine out each of the selected domains was modified due to the required scale of computing resources. Prior data indicate that domains may contain more than one modification, which raises the question of the nature of the changes incurred by modifying a different nearby lysine or more than one lysine within a single domain. It is difficult to predict the precise consequences of this without further modeling. We hypothesize that the modification of two lysines in a single domain, if they participate in salt bridge formation, would impact on tropoelastin structure. To test this hypothesis, various combinations of allysines could be incorporated into future molecular dynamics studies.

Taken together, our data reveal that allysines can cause global changes in structure, domain mobility and overall molecular motions of tropoelastin, and so contribute to irreversible cross-linked aggregates in hierarchical elastin assembly.

Acknowledgements

A.S.W. acknowledges funding from the Australian Research Council, National Health & Medical Research Council and the Cell Therapy Manufacturing Cooperative Research Centre. J.O. acknowledges funding from the University of Sydney Postgraduate Awards and scholarship top-up from the Cell Therapy Manufacturing Cooperative Research Centre. R.W. acknowledges an Australian Postgraduate Award and Australian Government Research Training Program Stipend Scholarship.

This work was supported by multiple high computing facilities. The authors acknowledge the Sydney Informatics Hub and the University of Sydney's high-performance computing cluster Artemis, and the National Computational Infrastructure (NCI), which is supported by the Australian Government.

This work also utilized the Extreme Science and Engineering Discovery Environment (XSEDE) [44], which is supported by National Science Foundation grant number ACI-1053575. XSEDE resources Stampede 2 and Ranch at the Texas Advanced Computing Center and Comet at the San Diego Supercomputing Center through allocations TG-MSS090007 and TG-MCB180008. This work was further supported by ONR DURIP N00014-17-1-2320, ONR N000141612333 and NIH 5U01EB014976.

Competing interests

The authors declare no competing interest. A.S.W. is the Scientific Founder of Elastagen Pty Ltd., which was recently sold to Allergan plc.

Author contributions

J.O. conceptualized experiments, conducted allysine studies, curated data, provided analysis scripts, conducted data analysis, and wrote and edited the manuscript.

A.T. conceptualized the experiments, provided WT data, provided analysis scripts, contributed to data analysis and edited the manuscript.

R.W. contributed to data analysis, provided analysis scripts, and wrote and edited the manuscript.

M.J.B. supervised the study, provided resources, conceptualized the experiments, provided WT data, contributed to data analysis, and edited the manuscript.

A.S.W. supervised the study, provided resources, conceptualized experiments, conducted allysine studies, contributed to data analysis and wrote and edited the manuscript.

Appendix A. Supplementary data

Supplementary data to this article can be found online at https://doi.org/10.1016/j.mbplus.2019.03.001.

Received 17 January 2019;
Received in revised form 10 March 2019;
Accepted 10 March 2019
Available online 12 March 2019

Keywords:
Elastin;
Assembly;
Molecular dynamics;
Replica exchange molecular dynamics

Abbreviations used:
ECM, extracellular matrix; LNL, lysinonorleucine; ALL, allysine aldol; MD, molecular dynamics; REMD, replica exchange molecular dynamics; ANM, anisotropic network model; NMA, normal mode analysis; PCA, principal component analysis; WT, wild type tropoelastin; ALK353, tropoelastin containing allysine at residue 353; ALK353, tropoelastin containing allysine at residue 507; 5ALK, tropoelastin containing 5 allysine residues; RMSD, root mean square deviation; SASA, solvent accessible surface area.

References

[1] G.C. Yeo, F.W. Keeley, A.S. Weiss, Coacervation of tropoelastin, Advances in Colloid and Interface Science 167 (2011) 94–103.

[2] M.L. Duque Lasio, B.A. Kozel, Elastin-driven genetic diseases, Matrix Biology 71-72 (2018) 144–160.

[3] N.A. Saunders, M.E. Grant, Elastin biosynthesis in chick-embryo arteries. Studies on the intracellular site of synthesis of tropoelastin, Biochemical Journal 221 (1984) 393–400.

[4] I. Pasquali-Ronchetti, M. Baccarani-Contri, C. Fornieri, G. Mori, D. Quaglino, Structure and composition of the elastin fibre in normal and pathological conditions, Micron 24 (1993) 75–89.

[5] B.A. Kozel, B.J. Rongish, A. Czirok, J. Zach, C.D. Little, E.C. Davis, R.H. Knutsen, J.E. Wagenseil, M.A. Levy, R.P. Mecham, Elastic fiber formation: a dynamic view of extracellular matrix assembly using timer reporters, Journal of Cellular Physiology 207 (2006) 87–96.

[6] A.W. Clarke, E.C. Arnspang, S.M. Mithieux, E. Korkmaz, F. Braet, A.S. Weiss, Tropoelastin massively associates during coacervation to form quantized protein spheres, Biochemistry 45 (2006) 9989–9996.

[7] Y. Fukuda, N. Nakazawa, N. Yamanaka, Interactions of elastin and microfibrils in elastogenesis of human pulmonary fibroblasts in culture, Connective Tissue Research 29 (1993) 301–310.

[8] H.M. Kagan, K.A. Sullivan, Lysyl oxidase: preparation and role in elastin biosynthesis, Methods in Enzymology. 82 Pt A (1982) 637–650.

[9] F. Sato, R. Seino-Sudo, M. Okada, H. Sakai, T. Yumoto, H. Wachi, Lysyl oxidase enhances the deposition of Tropoelastin through the catalysis of Tropoelastin molecules on the cell surface, Biological & Pharmaceutical Bulletin 40 (2017) 1646–1653.

[10] R.P. Mecham, Elastin in lung development and disease pathogenesis, Matrix Biology 73 (2018) 6–20.

[11] R.C. Siegel, S.R. Pinnell, G.R. Martin, Cross-linking of collagen and elastin. Properties of lysyl oxidase, Biochemistry 9 (1970) 4486–4492.

[12] S.R. Pinnell, G.R. Martin, The cross-linking of collagen and elastin: enzymatic conversion of lysine in peptide linkage to alpha-aminoadipic-delta-semialdehyde (allysine) by an extract from bone, Proceedings of the National Academy of Sciences of the United States of America 61 (1968) 708–716.

[13] S.M. Partridge, Biosynthesis and nature of elastin structures, Federation Proceedings 25 (1966) 1023–1029.

[14] S.M. Partridge, D.F. Elsden, J. Thomas, A. Dorfman, A. Telser, P.L. Ho, Biosynthesis of the desmosine and isodesmosine cross-bridges in elastin, Biochemical Journal 93 (1964) 30C–33C.

[15] S.M. Mithieux, Y. Tu, E. Korkmaz, F. Braet, A.S. Weiss, In situ polymerization of tropoelastin in the absence of chemical cross-linking, Biomaterials 30 (2009) 431–435.

[16] C.U. Schrader, A. Heinz, P. Majovsky, B. Karaman Mayack, J. Brinckmann, W. Sippl, C.E.H. Schmelzer, Elastin is heterogeneously cross-linked, The Journal of Biological Chemistry 293 (2018) 15107–15119.

[17] G.C. Yeo, A. Tarakanova, C. Baldock, S.G. Wise, M.J. Buehler, A.S. Weiss, Subtle balance of tropoelastin molecular shape and flexibility regulates dynamics and hierarchical assembly, Science Advances 2 (2016), e1501145.

[18] A. Tarakanova, G.C. Yeo, C. Baldock, A.S. Weiss, M.J. Buehler, Molecular model of human tropoelastin and implications of associated mutations, Proceedings of the National Academy of Sciences of the United States of America 115 (2018) 7338–7343.

[19] S. Rauscher, R. Pomes, The liquid structure of elastin, eLife 6 (2017), e26526.

[20] G.C. Yeo, C. Baldock, S.G. Wise, A.S. Weiss, A negatively charged residue stabilizes the tropoelastin N-terminal region for elastic fiber assembly, The Journal of Biological Chemistry 289 (2014) 34815–34826.

[21] G.C. Yeo, C. Baldock, A. Tuukkanen, M. Roessle, L.B. Dyksterhuis, S.G. Wise, J. Matthews, S.M. Mithieux, A.S. Weiss, Tropoelastin bridge region positions the cell-interactive C terminus and contributes to elastic fiber assembly, Proceedings of the National Academy of Sciences of the United States of America 109 (2012) 2878–2883.

[22] P. Lee, D.V. Bax, M.M. Bilek, A.S. Weiss, A novel cell adhesion region in tropoelastin mediates attachment to integrin alphaVbeta5, The Journal of Biological Chemistry 289 (2014) 1467–1477.

[23] P. Brown-Augsburger, C. Tisdale, T. Broekelmann, C. Sloan, R.P. Mecham, Identification of an elastin cross-linking domain that joins three peptide chains. Possible role in nucleated assembly, The Journal of Biological Chemistry 270 (1995) 17778–17783.

[24] A. Heinz, C.U. Schräder, S. Baud, F.W. Keeley, S.M. Mithieux, A.S. Weiss, R.H.H. Neubert, C.E.H. Schmelzer, Molecular-level characterization of elastin-like constructs and human aortic elastin, Matrix Biology 38 (2014) 12–21.

[25] S.G. Wise, S.M. Mithieux, M.J. Raftery, A.S. Weiss, Specificity in the coacervation of tropoelastin: solvent exposed lysines, Journal of Structural Biology 149 (2005) 273–281.

[26] S.M. Mithieux, S.G. Wise, M.J. Raftery, B. Starcher, A.S. Weiss, A model two-component system for studying the architecture of elastin assembly in vitro, Journal of Structural Biology 149 (2005) 282–289.

[27] A. Tarakanova, G.C. Yeo, C. Baldock, A.S. Weiss, M.J. Buehler, Tropoelastin is a flexible molecule that retains its canonical shape, Macromolecular Bioscience 1800250 (2018) 1–7.

[28] S.G. Wise, G.C. Yeo, M.A. Hiob, J. Rnjak-Kovacina, D.L. Kaplan, M.K. Ng, A.S. Weiss, Tropoelastin: a versatile, bioactive assembly module, Acta Biomaterialia 10 (2014) 1532–1541.

[29] C. Baldock, A.F. Oberhauser, L. Ma, D. Lammie, V. Siegler, S.M. Mithieux, Y. Tu, J.Y. Chow, F. Suleman, M. Malfois, S. Rogers, L. Guo, T.C. Irving, T.J. Wess, A.S. Weiss, Shape of tropoelastin, the highly extensible protein that controls human tissue elasticity, Proceedings of the National Academy of Sciences of the United States of America 108 (2011) 4322–4327.

[30] A. Bakan, L.M. Meireles, I. Bahar, ProDy: protein dynamics inferred from theory and experiments, Bioinformatics (Oxford, England) 27 (2011) 1575–1577.

[31] A.D. MacKerell Jr., D. Bashford, M. Bellott, R.L. Dunbrack Jr., J.D. Evanseck, M.J. Field, S. Fischer, J. Gao, H. Guo, S. Ha, All-atom empirical potential for molecular modeling and dynamics studies of proteins, The Journal of Physical Chemistry. B 102 (1998) 3586–3616.

[32] K. Vanommeslaeghe, E. Hatcher, C. Acharya, S. Kundu, S. Zhong, J. Shim, E. Darian, O. Guvench, P. Lopes, I. Vorobyov, A.D. Mackerell Jr., CHARMM general force field:

a force field for drug-like molecules compatible with the CHARMM all-atom additive biological force fields, Journal of Computational Chemistry 31 (2010) 671–690.
[33] W. Humphrey, A. Dalke, K. Schulten, VMD: visual molecular dynamics, Journal of Molecular Graphics 14 (1996) 33–38 (27-8).
[34] J.C. Phillips, R. Braun, W. Wang, J. Gumbart, E. Tajkhorshid, E. Villa, C. Chipot, R.D. Skeel, L. Kale, K. Schulten, Scalable molecular dynamics with NAMD, Journal of Computational Chemistry 26 (2005) 1781–1802.
[35] M. Feig, J. Karanicolas, C.L. Brooks 3rd, MMTSB tool set: enhanced sampling and multiscale modeling methods for applications in structural biology, Journal of Molecular Graphics & Modelling 22 (2004) 377–395.
[36] S.M. Mithieux, S.G. Wise, A.S. Weiss, Tropoelastin—a multifaceted naturally smart material, Advanced Drug Delivery Reviews 65 (2013) 421–428.
[37] D.V. Bax, U.R. Rodgers, M.M. Bilek, A.S. Weiss, Cell adhesion to tropoelastin is mediated via the C-terminal GRKRK motif and integrin alphaVbeta3, The Journal of Biological Chemistry 284 (2009) 28616–28623.
[38] T.J. Broekelmann, B.A. Kozel, H. Ishibashi, C.C. Werneck, F. W. Keeley, L. Zhang, R.P. Mecham, Tropoelastin interacts with cell-surface glycosaminoglycans via its COOH-terminal domain, The Journal of Biological Chemistry 280 (2005) 40939–40947.
[39] A. Tarakanova, W. Huang, A.S. Weiss, D.L. Kaplan, M.J. Buehler, Computational smart polymer design based on elastin protein mutability, Biomaterials 127 (2017) 49–60.
[40] Z. Urban, J. Zhang, E.C. Davis, G.K. Maeda, A. Kumar, H. Stalker, J.W. Belmont, C.D. Boyd, M.R. Wallace, Supravalvular aortic stenosis: genetic and molecular dissection of a complex mutation in the elastin gene, Human Genetics 109 (2001) 512–520.
[41] S.E. Reichheld, L.D. Muiznieks, F.W. Keeley, S. Sharpe, Direct observation of structure and dynamics during phase separation of an elastomeric protein, Proceedings of the National Academy of Sciences of the United States of America 114 (2017) E4408–E4415.
[42] L.B. Dyksterhuis, A.S. Weiss, Homology models for domains 21–23 of human tropoelastin shed light on lysine cross-linking, Biochemical and Biophysical Research Communications 396 (2010) 870–873.
[43] B. Vrhovski, S. Jensen, A.S. Weiss, Coacervation characteristics of recombinant human tropoelastin, European Journal of Biochemistry 250 (1997) 92–98.
[44] J. Towns, T. Cockerill, M. Dahan, I. Foster, K. Gaither, A. Grimshaw, V. Hazelwood, S. Lathrop, D. Difka, G.D. Peterson, R. Roskies, J.R. Scott, N. Wilkens-Diehr, XSEDE: accelerating scientific discovery, Computing in Science & Engineering 16 (2014) 62–74.